IMPEDANCES OF BELLOWS CORRUGATIONS

King-Yuen Ng
Fermi National Accelerator Laboratory†, *Batavia, IL 60510*

I. INTRODUCTION

The longitudinal and transverse coupling impedances of inner bellows can be derived by running[1] TBCI and taking Fourier transforms[2,3]. However, the eventual impedance plots are only very approximate because the results are usually marred by errors due to the finite mesh size and the truncation of the wake potentials. It has been reported that TBCI gives results in conflict with other codes[4,5] like KN7C and TRANSVRS. Also, a long wake for a simple pill-box cavity even diverges in the dipole mode. In this paper, we want to present a physical understanding of the impedance plots and try to gather some formulae so that the main features of the impedances can be approximately derived without the actual running of any time-consuming codes. Similar attempts have also been made in Ref 2.

II. ONE CORRUGATION

Consider one *rectangular* corrugation of the bellows having a depth Δ and half width g. Henke[6] has studied the problem in the frequency domain, which involves the solution of an infinite matrix equation. However, when $g/b \ll 1$, where b is the beam pipe radius, the longitudinal impedance can be simplified tremendously[7]:

$$Z_{\parallel}(\omega) = \frac{gZ_0}{\pi b I_0^2(\bar{b}) D}, \tag{2.1}$$

where

$$D = j\frac{R_0'(kb)}{R_0(kb)} - 2kj\left[\sum_{s=1}^{S}\frac{1}{\beta_s^2}\left(1 - e^{-j\beta_s g}\frac{\sin\beta_s g}{\beta_s g}\right) - \sum_{s=S+1}^{\infty}\frac{1}{\alpha_s^2}\left(1 - e^{-\alpha_s g}\frac{\sinh\alpha_s g}{\alpha_s g}\right)\right]. \tag{2.2}$$

In the above, $k = \omega/c$, $Z_0 = 377\ \Omega$, I_0 is the modified Bessel function of order zero, $\bar{b} = bk/\gamma\beta$, γ and β are the relativistic velocity parameters of the beam particles. In the summations, $\beta_s = \sqrt{k^2b^2 - j_{0s}^2}$ and $\alpha_s = \sqrt{j_{0s}^2 - k^2b^2}$, where j_{0s} is the s-th zero of the Bessel function J_0 and j_{0S} is the zero that is just larger or equal to kb. Also, $R(kb) = J_0(kb)N_0(kd) - J_0(kd)N_0(kb)$, where $d = b + \Delta$ and J_0 and N_0 are respectively the Bessel function and Neumann function of order zero. To have a deeper insight, let us take the limit $kb \gg 1$ and $g/b \to 0$; D is simplified to

$$D = -j\cot k\Delta - \sum_{s=1}^{S}\frac{2kg}{\sqrt{k^2b^2 - j_{0s}^2}} + \sum_{s=S+1}^{\infty}\frac{2jkg}{\sqrt{j_{0s}^2 - k^2b^2}}. \tag{2.3}$$

Here, in reality, the second summation cannot go to infinity because the expansion will break down as soon as $\alpha_s g \simeq 1$.

The zeroes of $Im\,D$ determines the peaks of resonances. If the summations are neglected, from Eq. (2.3), sharp resonances occur at $k\Delta = \pi/2,\ 3\pi/2$, etc.; or when the depth Δ is an odd number of the quarter wavelength. Take the case of a corrugation depth of $\Delta = 5$ mm, $\cot k\Delta$ gives resonances at $15, 45, 75, \ldots$ GHz. Thus, usually only the first one will be visible to the beam. The first summation in D represents all the above-cutoff modes of waves that can propagate along the beam pipe so that the sharp resonances will be damped heavily. The second summation which is imaginary represents all the below-cutoff modes that attenuate along the beam pipe. Its effect can be thought of as fields clinging to the opening of the corrugation, thus making the corrugation depth Δ effectively longer and the resonance frequencies smaller. Figure 1 shows the plot of $Z_{\parallel}$ due to a corrugation of depth $\Delta/b = 0.1$ and half width $g/b = 0.025$. We see a broad resonance with the resonant frequency shifted from $kb = \pi b/\Delta = 15.7$ to ~ 13. We also see notches located exactly at $kb = j_{0s}$, the zeroes of J_0 or the cutoff frequencies of the pipe. These notches are evident from Eq. (2.3) where only one term in the summation will contribute. Physically, since $2g \ll \lambda$, the wavelength, only the z-independent mode is favored in the region of the corrugation. At one of the cutoff frequencies, the mode that is just allowed is z-independent and is therefore favored and dominates all others. This mode will not penetrate into the corrugation at all and, as a result, the beam does not see the corrugation. The plot also shows some sharp resonances just before the cutoff dips at frequencies below the broad resonance peak. According to Henke, they belong to some well-trapped modes in the region of the cross section enlargement.

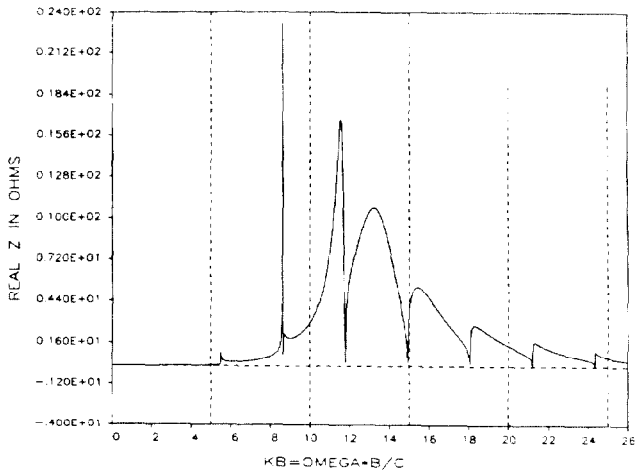

Figure 1: Real part of the longitudinal impedance of one corrugation of a bellows with half width $g/b = 0.025$ and depth $\Delta/b = 0.1$.

For a bellows with many corrugations, we expect the notches and sharp peaks to smooth out. This happens because the total length of the bellows is no longer negligibly small compared with the beam pipe radius; so the z-independent mode is no longer favored. With the corrugations closely spaced, fields will cling across several corrugations resulting in further lengthening the effective corrugation depth and thus further lowering the broad-band frequency. The overall picture of the longitudinal impedance is therefore a broad band resonance derived from the first resonance in the corrugation. We can characterize it by the resonant angular frequency ω_r, the shunt impedance $R_{\parallel}$ and the quality factor Q; *i.e.*,

$$Z_{\parallel}(\omega) = \frac{R_{\parallel}}{1 - jQ\left(\frac{\omega_r}{\omega} - \frac{\omega}{\omega_r}\right)}. \tag{2.4}$$

It is a good approximation to assume that the position of the broad band and its Q-value are not altered much. They can

†Operated by the Universities Research Association, Inc., under contract with the U. S. Department of Energy.

CH2387-9/87/0000-1051 $1.00 © IEEE

therefore be estimated using Eq. (2.2) and possibly Eq. (2.3):

$$Im\, D(k_r b) = 0, \qquad Q \sim \frac{kb}{2\, Re\, D} \frac{d\, Im\, D}{d(kb)}\Big|_{kb=k_r b}, \tag{2.5}$$

which gives Q from 3 to 8 for the examples studied below. We should not expect this formula to be accurate at all due to the notches and sharp peaks, but it does tell us that $Q \sim 5$.

The transverse impedance, on the other hand, behaves similarly and can be expressed as

$$Z_\perp(\omega) = \frac{\omega}{\omega_r} \frac{R_\perp}{1 - jQ\left(\frac{\omega_r}{\omega} - \frac{\omega}{\omega_r}\right)}, \tag{2.6}$$

The position of the broad band should be roughly the same as that of the longitudinal impedance. This can be understood by considering the bellows corrugation as a radial transmission line. The resonant frequency is therefore roughly proportional to $c\sqrt{(1/4\Delta)^2 + (1/2\pi b)^2}$. Since $(2\pi b)^2 \gg (4\Delta)^2$ in most cases, the resonant frequency is dominated by Δ only.

Inner bellows of various sizes are examined. The results are shown in Table 1. The TBCI values are for 5 corrugations while the Henke values are for one only using Eq. (2.5). We see that the TBCI values are indeed roughly the same for the longitudinal and transverse situations, but they are slightly lower than the Henke values as expected. The agreement is roughly 10% except for Case 11 which has a corrugation depth of only 0.25 cm, the most shallow among the others. Therefore, the resonant frequency will be very sensitive to the lengthening of the depth by the fields clinging to the opening. Comparing Cases 8, 14 and 15, we learn that the change in resonant frequency f_r depends very weakly on the corrugation gap g. A 100% increase in g lowers f_r by 9% only. If this dependence on g is neglected, we can obtain a fitted relation shown in Fig. 2,

$$k_r b = 1.37 \left(\frac{\Delta}{b}\right)^{-0.948}, \tag{2.7}$$

where $k_r = 2\pi f_r/c$. The fit is a very good one except for Cases 11 and 13. The former may be a result of the shallowness of the corrugation. The latter is the one with $\Delta/b = 0.5$ which is the biggest of all cases. Thus, we may conclude that Eq. (2.7) holds for corrugation with $\Delta/b < 0.5$ and $\Delta > 0.25$ cm. Similar fit for $Z_\perp$ has been done[2] using TRANSVRS but the results differ from the above. This empirical formula can also be written as

$$k_r \Delta = 1.37 \left(\frac{\Delta}{b}\right)^{0.052}. \tag{2.8}$$

Since the exponent is small, Eq. (2.8) just says that the fields due to the cutoff modes lower $k_r\Delta$ from $\pi/2 = 1.57$ to 1.37.

III. LOW-FREQUENCY BEHAVIORS

The ratios of shunt impedances to quality factors are related to the low-frequency behaviors of the impedances. From Eqs. (2.4) and (2.6), we get, at zero frequency,

$$\frac{Im\, Z_\parallel}{f} = \frac{2\pi R_\parallel}{\omega_r Q} \quad \text{and} \quad Im\, Z_\perp = \frac{R_\perp}{Q}. \tag{3.1}$$

On the other hand, from the low-frequency magnetic field trapped inside a narrow cavity, we obtain[8],

$$\frac{Z_\parallel}{f} = j\frac{2gZ_0}{c} \ln S \quad \text{and} \quad Z_\perp = j\frac{2gZ_0}{\pi b^2} \frac{S^2 - 1}{S^2 - 1}, \tag{3.2}$$

where $Z_0 = 377\ \Omega$, R the ring radius, and $S = 1 + \Delta/b$. These formulae are compared with the TBCI results in Table 2.

Case No.	b	Δ	$2g$	f_r in GHz		
	cm	cm	cm	Henke	TBCI($\parallel$)	TBCI($\perp$)
1	1.50	0.50	0.15	13.3	12.3	12.3
2	2.00	0.50	0.15	12.2	11.5	12.2
3	2.75	0.50	0.15	12.9	11.8	11.6
4	3.25	0.50	0.15	12.2	11.6	11.9
5	3.50	0.50	0.15	13.1	11.7	11.8
6	4.50	0.50	0.15	12.1	11.6	11.8
7	6.15	0.50	0.15	13.1	11.4	11.6
8	6.50	0.50	0.15	12.6	11.4	11.6
9	8.00	0.50	0.15	12.3	11.6	11.3
10	2.00	0.50	0.20	11.9	11.2	11.5
11	2.00	0.25	0.15	24.1	21.0	21.0
12	2.00	0.75	0.15	9.4	8.3	8.3
13	2.00	1.00	0.15	7.4	7.0	7.0
14	6.50	0.50	0.20	12.3	10.8	10.9
15	6.50	0.50	0.30	12.0	10.2	10.3

Table 1: Resonance frequencies of various bellows configurations.

IV. ENERGY LOSS

For a Gaussian bunch of RMS length σ_ℓ, the rate of loss of energy is proportional to the energy loss factor $k_\parallel$ defined as

$$k_\parallel = \frac{1}{\pi} \int_0^\infty d\omega e^{-(\omega\sigma_\ell/c)^2}\, Re\, Z_\parallel(\omega). \tag{4.1}$$

With Eq. (2.4) as the expression for the longitudinal impedance, Eq. (4.1) can be integrated in the closed form to give for *one* corrugation of the bellows[9],

Case	b	Δ	$2g$	$Im\, Z_\parallel/f$ (Ω/GHz)		$Im\, Z_\perp$ (Ω/m)	
	cm	cm	cm	Eq. (3.2)	TBCI	Eq. (3.2)	TBCI
1	1.50	0.50	0.15	0.542	0.540	224	199
2	2.00	0.50	0.15	0.410	0.410	98.8	89.6
3	2.75	0.50	0.15	0.315	0.310	39.4	36.0
4	3.25	0.50	0.15	0.269	0.270	24.2	22.4
5	3.50	0.50	0.15	0.252	0.256	19.5	18.4
6	4.50	0.50	0.15	0.199	0.202	9.33	8.88
7	6.15	0.50	0.15	0.150	0.147	3.71	3.54
8	6.50	0.50	0.15	0.140	0.140	3.15	3.7
9	8.00	0.50	0.15	0.117	0.117	1.70	1.64
10	2.00	0.50	0.20	0.561	0.556	132	116
11	2.00	0.25	0.15	0.222	0.221	52.8	46.7
12	2.00	0.75	0.15	0.600	0.600	139	124
13	2.00	1.00	0.15	0.764	0.720	173	155
14	6.50	0.50	0.20	0.186	0.190	4.20	3.94
15	6.50	0.50	0.30	0.280	0.277	6.30	5.70

Table 2: $Im\, Z_\parallel/f$ and $Im\, Z_\perp$ per corrugation at zero frequency.

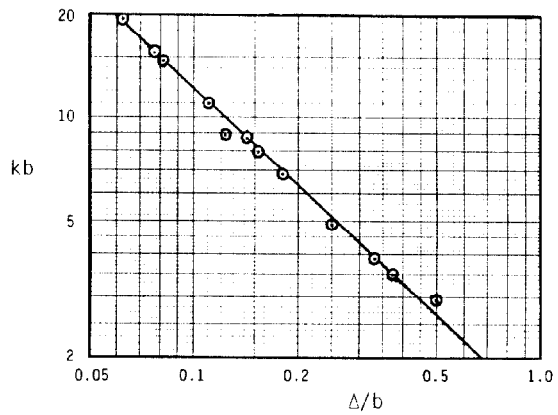

Figure 2: A fit of the resonance position as a function of Δ/b.

$$k_{\parallel} = \frac{R_{\parallel}\omega_r}{2Q\alpha}\left(1 - \frac{1}{4Q^2}\right)^{-1/2} \mathcal{R}e[zw(z)], \qquad (4.2)$$

with $\alpha = \omega_r\sigma_\ell/c$, $z = (\sqrt{1 - 1/4Q^2} + j/2Q)\alpha$ and $w(z)$ the complex error function. For a very short bunch, $\alpha \to 0$, we have $w(z) = 1 + 2jz/\sqrt{\pi} - z^2$; or

$$k_{\parallel} = \frac{R_{\parallel}\omega_r}{2Q}\left(1 - \frac{2\alpha}{\sqrt{\pi}Q}\right), \qquad (4.3)$$

which is nothing but the area under one resonance divided by π. For a very long bunch, $\alpha \to \infty$, we have $w(z) = j(1 + 1/2z^2)/\sqrt{\pi}z$; so

$$k_{\parallel} = \frac{R_{\parallel}\omega_r}{4\sqrt{\pi}Q^2\alpha^3}. \qquad (4.4)$$

The smallness of $k_{\parallel}$ is due to the exponential factor and the fact that $\mathcal{R}e\, Z_{\parallel}$ starts off from zero and rises only near the broad resonance.

For the Superconducting Super Collider (SSC), $\sigma_\ell = 7$ cm. If the corrugations have a depth of 0.5 cm, period 0.30 cm and are of inner bellows configuration having a beam pipe radius of 1.65 cm, the broad resonance is at $\sim$ 12.3 GHz, according to Eq. (2.7). Using Eqs. (3.1) and (3.2), one gets $R_{\parallel}/Q = 6.14\ \Omega$ for each corrugation. The parameter $\alpha = \omega_r\sigma_\ell/c = 18.0$, so Eq. (4.4) can be used. The energy loss is therefore $k_{\parallel} = 1.14 \times 10^7/Q\ \Omega$/sec for one corrugation. In the SSC, there are 1.2 km of bellows or 400,000 corrugations and 17,280 bunches each with 7.3×10^9 particles. The revolution frequency is 3.614 kHz. Thus, the energy loss is $389/Q$ or 78 watts if $Q \sim 5$.

For the transverse impedance, there is a similar loss factor

$$k_{\perp} = \frac{1}{2\pi j}\int_{-\infty}^{\infty} d\omega Z_{\perp}(\omega) e^{-(\omega\sigma_\ell/c)^2}, \qquad (4.5)$$

where a Gaussian bunch has been assumed. Using Eq. (2.4), the integral can be done in the closed form:

$$k_{\perp} = \frac{R_{\perp}\omega_r}{2Q}\left(1 - \frac{1}{4Q^2}\right)^{-1/2} \mathcal{I}m\, w(z). \qquad (4.6)$$

For a very short bunch, we get $k_{\perp} = R_{\perp}\omega_r\alpha/\sqrt{\pi}Q$. When the bunch is very long, $k_{\perp} = R_{\perp}\omega_r/(2\sqrt{\pi}Q\alpha)$. The general shapes of $k_{\parallel}$ and $k_{\perp}$ are plotted in Fig. 3, and listed with the TBCI results in Table 3. The agreement is satisfactory.

Case	b	Δ	$2g$	$k_{\parallel}$		$k_{\perp}$	
	cm	cm	cm	Eq. (4.2)	TBCI	Eq. (4.6)	TBCI
1	1.50	0.50	0.15	0.782	0.700	44.6	45.4
2	2.00	0.50	0.15	0.591	0.534	19.9	18.4
3	2.75	0.50	0.15	0.454	0.390	7.86	7.06
4	3.25	0.50	0.15	0.388	0.332	4.87	4.30
5	3.50	0.50	0.15	0.363	0.312	3.92	3.46
6	4.50	0.50	0.15	0.287	0.244	1.86	1.66
7	6.15	0.50	0.15	0.216	0.178	0.73	0.66
8	6.50	0.50	0.15	0.201	0.169	0.62	0.56
9	8.00	0.50	0.15	0.168	0.139	0.33	0.30
10	2.00	0.50	0.20	0.805	0.696	25.6	23.4
11	2.00	0.25	0.15	0.177	0.164	13.1	11.5
12	2.00	0.75	0.15	0.707	0.650	18.8	11.5
13	2.00	1.00	0.15	0.745	0.666	18.4	19.5
14	6.50	0.50	0.20	0.263	0.220	0.78	0.70
15	6.50	0.50	0.30	0.386	0.308	1.10	0.95

Table 3: $k_{\parallel}$ in $10^{11}\ \Omega$/sec and $k_{\perp}$ in $10^{11}\ \Omega$/m/sec per corrugation. RMS bunch length is 4 mm and $Q = 5$.

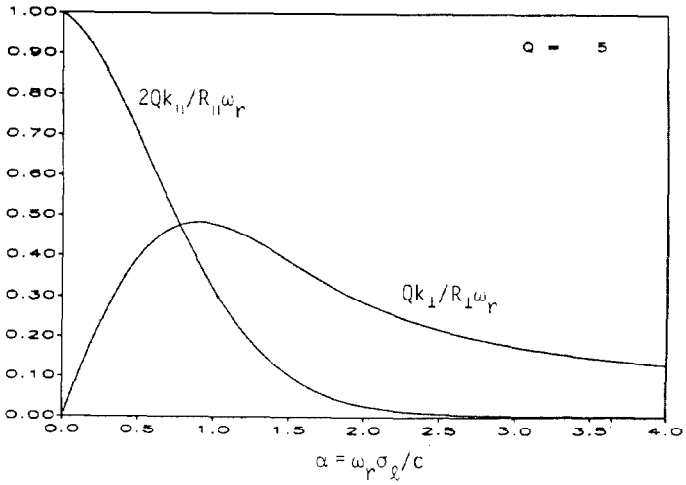

Figure 3: Plot of $k_{\parallel}$ and $k_{\perp}$ versus $\alpha = \omega_r\sigma_\ell/c$.

V. MANY CORRUGATIONS

We have examined the situations of 1, 5, 20 and 40 corrugations each of depth $\Delta = 0.5$ cm, period $4g = 0.3$ cm, with beam pipe radius $b = 2.0$ cm, and RMS bunch length $\sigma_\ell = 4$ mm. The TBCI results are listed in Table 4. We see that resonant frequencies are lower with more corrugations as anticipated. The transverse loss factor $k_{\perp}$ also decreases with more corrugations. However, it is interesting to see that $\mathcal{I}m\, Z_{\parallel}/f$, $\mathcal{I}m\, Z_{\perp}$ and $k_{\parallel}$ are almost independent of the number of corrugations. These are in fact the quantities used in the study of single-bunch and coupled-bunch instabilities as well as parasitic heating. In order words, we can safely use the formulae developed in the previous sections to compute these quantities per corrugation, multiply them by the number of corrugations in the ring, and use the final results in the stability criteria and parasitic energy loss formula.

n	$f_{r\parallel}$ GHz	$f_{r\perp}$ GHz	$\mathcal{I}m\, Z_{\parallel}/f$ Ω/GHz	$\mathcal{I}m\, Z_{\perp}$ Ω/m	$k_{\parallel}$ $10^{11}\Omega$/sec	$k_{\perp}$ $10^{11}\Omega$/m/sec
1	12.1	13.2	0.413	85.8	0.561	22.3
5	11.5	12.2	0.410	89.6	0.534	19.9
20	10.0	10.3	0.407	83.4	0.520	16.7
40	9.0	9.7	0.414	86.5	0.530	16.0

Table 4: The resonant frequencies, impedances at zero frequency and loss factors for $n = 1, 5, 20, 40$ corrugations. All values shown are per corrugation. Each corrugation has a depth of 5 mm and period 3 mm. The beam pipe radius is 2 cm and the RMS bunch length 4 mm.

References

[1] T. Weiland, DESY Report 82-015 (1982).

[2] K. Bane and R. Ruth, SSC Central Design Group Report No. SSC-SR-1017, p. 10.

[3] J. Bisognano and K. Ng, *ibib*, p. 45.

[4] E. Keil, Nucl. Instr. and Meth., **100**, 419 (1972).

[5] K. Bane and B. Zotter, Proceedings of the 11th Int. Conf. on High Energy Accelerators, CERN (1980), p. 580.

[6] H. Henke, CERN Report CERN-LEP-RF/85-41.

[7] R. L. Gluckstern, private communication.

[8] E. Keil and W. Zotter, Particle Accelerator **3**, 11 (1972); K. Y. Ng, Fermilab Report FN-389.

[9] M. Furman, SSC Central Design Group Report SSC-N-142 (1986).